CHEMISTRY OF MATERIALS

ARTICLE

pubs.acs.org/cm

Hydrothermal Synthesis of Manganese Oxide Nanomaterials and Their Catalytic and Electrochemical Properties

Guohong Qiu,[†,‡] Hui Huang,[‡] Saminda Dharmarathna,[‡] Evan Benbow,[‡] Lisa Stafford,[‡] and Steven L. Suib[‡]

[†]Key Laboratory of Subtropical Agriculture Resources and Environment, Ministry of Agriculture, College of Resources and Environment, Huazhong Agricultural University, Wuhan, 430070, P. R. China

[‡]Department of Chemistry, University of Connecticut, Storrs, 55 North Eagleville Road, Storrs, Connecticut, 06269, United States

Supporting Information

ABSTRACT: Manganese oxides were fabricated by hydrothermal reactions of $KMnO_4$ and $MnSO_4$ solutions. Crystal structures and morphologies of samples were characterized by X-ray diffraction, scanning electron microscopy, Brunauer–Emmett–Teller (BET) measurements, Fourier transform infrared spectroscopy, and thermogravimetric analysis. The combined effects of temperature, additives of H_2SO_4, and tetrabutylammonium bromide (TBAB) on manganese oxide crystal structures were investigated. The key factors affecting catalytic activity and electrochemical performance of manganese oxides were studied using oxidation of benzyl alcohol and cyclic voltammetry, respectively. The results indicated that pyrolusite (OMS-7) was formed in 0.1 mol·L^{-1} $MnSO_4$ solution with $KMnO_4/MnSO_4$ molar ratios of 7:18 and 8:17 at 120 °C, respectively. A mixture of OMS-7 and cryptomelane (OMS-2) was prepared when the molar ratio increased. Potassium ion plays an important role in the formation of OMS-2. Steric effects arose from complexation reactions of TBAB and $MnSO_4$ solutions and facilitated the formation of OMS-2. K-OMS-2 and H-K-OMS-2 were formed by adding 0.1 mol·L^{-1} TBAB and 0.2 mol·L^{-1} H_2SO_4 to 0.1 mol·L^{-1} $MnSO_4$ solution with a $KMnO_4/MnSO_4$ molar ratio of 11:14 at 120 °C, respectively. The catalytic oxidation activity was found to follow this trend: H-K-OMS-2 > K-OMS-2 > OMS-7 likely because of the larger amount of acid sites in H-K-OMS-2 . However, the exchangeable active oxygen and specific surface area had a greater impact on the electrochemical performance of manganese oxides. The electrocatalytic activity of synthesized manganese oxides for oxygen reduction increased in the order: OMS-7 < H-K-OMS-2 < K-OMS-2. Supercapacitor performance was compared, and the capacitance also increased in the sequence: OMS-7 < H-K-OMS-2 < K-OMS-2.

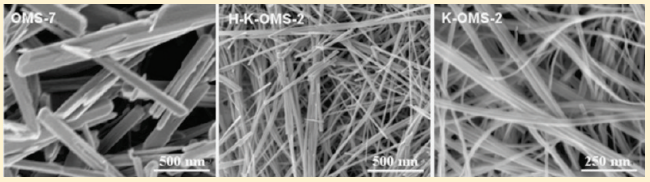

KEYWORDS: manganese oxide octahedral molecular sieves, cryptomelane, nanomaterials, hydrothermal reaction, catalysts, supercapacitor

1. INTRODUCTION

Manganese oxide octahedral molecular sieves (OMS) have attracted growing interest because of their unique fundamental properties and wide applications in the field of catalysis,[1−3] chemical sensing,[4] magnetism,[5,6] supercapacitors,[7,8] and lithium ion batteries[9] because of the low cost of raw materials, diversity of structures, low toxicity, and environmentally friendly characteristics. Tunnel structure manganese oxides are getting significant attention for their thermodynamic stability and high catalytic activity, especially for the 2 × 2 tunneled cryptomelane (OMS-2).[3,10,11] Usually, OMS-2 is prepared by the oxidation of Mn(II) salts or the reduction of Mn(VII) salts, and many oxidants and reductants have been chosen to control the microstructures and morpho logies during these above processes. The oxidants were reported to be $K_2Cr_2O_7$,[12] O_2,[13] $K_2S_2O_8$,[3,14,15] H_2O_2, $(NH_4)_2S_2O_8$ and NaClO,[15,16] etc. The reductants were hydrochloric acid,[5,11] graphite[8] and isoamyl alcohol,[17] and so forth. OMS-2 could also be formed from the transformation of birnessite.[18] However, in the experiments involving OMS-2, syntheses are usually performed by the redox reactions of $KMnO_4$ and $MnSO_4$ solutions under different conditions.[1,2,10,16,19−21]

For the fabrication of OMS-2, the molar ratio of $KMnO_4$ to $MnSO_4$, acidity, and temperature were important factors. In different experiments, various molar ratios of $KMnO_4$ and $MnSO_4$, acidity, and temperatures were used. DeGuzman et al. obtained OMS-2 using a molar ratio of 0.72 when the pH was 1.7 or lower at a temperature range of 100−120 °C, and pyrolusite (OMS-7) was formed when the temperature was higher than 120 °C.[19] On the basis of the above reactions, Makwana et al. prepared H-K-OMS-2 by ion-exchange of K-OMS-2 in a 1.0 mol·L^{-1} HNO_3 solution.[1] With a similar molar ratio, Schurz et al. prepared amorphous MnO_2 at room temperature.[20] Wang and Li systematically studied the influence of the molar ratio of $KMnO_4$ to $MnSO_4$ on manganese oxide structures without adjusting the pH of the system, and observed that OMS-2 was formed when the molar ratio of $KMnO_4/MnSO_4$ was kept at no less than 2.5:1, and increasing the ratio facilitated the formation of OMS-2 even at a higher temperature, such as 180 °C. When the ratio decreased to 2:3, OMS-7 was produced at

Received: April 24, 2011
Revised: July 1, 2011
Published: August 02, 2011

160 °C.[16] OMS-2 nanowires could also be synthesized using the reaction of $KMnO_4$ and $MnSO_4$ with a molar ratio of 2:3 by adjusting the pH ranging from 6.0 to 0 at 95 °C.[21] Although these studies made significant contributions to the synthesis of OMS-2 and other manganese oxides, few investigations have been focused on the hydrothermal synthesis of OMS-2 under the combined effect of the molar ratio of $KMnO_4$ to $MnSO_4$, acidity, and temperature, especially in the formation process. H-K-OMS-2 with a high catalytic activity should also be synthesized with a simplified one-step procedure.

Organic ammonium ions usually worked as effective additives during the synthesis of layered manganese oxide.[22−24] After the ion-exchange of H^+/K^+-OL-1 by tetraalkylammonium hydroxides, the interlayer distance of such materials increased remarkably, and many kinds of novel structures were observed.[22] On contact with aqueous TBA^+ ions, the layered manganese oxide underwent various reactions including intercalation, osmotic swelling, and delamination into single sheets.[23] Nakayama et al. electrochemically synthesized layered manganese oxides directly intercalated with tetraalkylammonium ions.[24] Tetraethylammonium bromide was used to complex with MnO_4^- to slow the reduction rate of MnO_4^- by Mn^{2+} to prepare a novel layered sodium manganese oxo-phosphate.[25] Tris(2-aminoethyl)amine was used as a template to synthesize layered manganese(II) phosphate $Mn_3(PO_4)_4 \cdot 2(H_3NCH_2CH_2)_3N \cdot 6H_2O$.[26] A coordination polymer can be used as a precursor to prepare γ-MnO_2.[27] When alkyl ammonium salts were used, they possibly work as complexing agents, template ions, and retardants during the preparation of manganese oxides by the hydrothermal reactions in the $KMnO_4$ and $MnSO_4$ solutions. However, the effect of additives of alkyl ammonium salts on the manganese oxide structures was seldom investigated.

Manganese oxides are well-known as active catalysts,[1−3,20] and exhibit high electrocatalytic performance for oxygen reduction.[11] The catalytic oxidation activity of the OMS-2 is related to its specific surface area, but exchangeable active oxygen and Lewis acid sites may play a more important role in the catalytic process,[1,20,28] which also affected the electrocatalytic activity of manganese oxides for methanol oxidation in fuel cells.[29] The electrochemical reduction process of oxygen on the surface of manganese oxides with different structures has been investigated.[11,30] However, the correlation between the exchangeable oxygen content and electrocatalytic reduction activity has not been definite at present. Manganese oxides have also been used for supercapacitors with wide application prospects.[7,8] The influence of microstructures, morphologies, specific surface areas, and conductivity on the specific capacitance was studied.[31,32] It is ambiguous whether exchangeable oxygen affected the electrochemical properties, especially for electrocatalytic reduction characteristics. Full understanding of the effect of exchangeable active oxygen and specific surface area on the electrochemical properties of manganese oxides with different structures can lead to the development of more effective catalysts and high-capacitance materials.

In this work, manganese oxide octahedral molecular sieves (OMS-7, K-OMS-2, and H-K-OMS-2) were fabricated by hydrothermal reactions of $KMnO_4$ and $MnSO_4$ solutions. The combined effects of molar ratios, sulfuric acid concentration, temperature, and tetrabutylammonium bromide (TBAB) on manganese oxide crystal structures were systematically studied. The exchangeable oxygen content was characterized by TGA, and the influence of specific surface area, the content of exchangeable active oxygen, and Lewis acid sites on the catalytic oxidation performance and electrochemical properties was compared and investigated via the oxidation of benzyl alcohol and cyclic voltammetry, respectively.

2. EXPERIMENTAL SECTION

2.1. Materials and Chemicals. $MnSO_4 \cdot H_2O$ (99%), tetramethylammonium bromide (TAB, ≥ 98%), tetrathylammonium bromide (TEAB, 99%), tetraoctylammonium bromide (TOAB, 98%), K_2SO_4 (≥99%), and Na_2SO_4 (>99%) were all purchased from Aldrich. $KMnO_4$ (>99%), tetrabutylammonium bromide (TBAB, ≥ 99%), and KOH (>87.8%) were supplied by ACROS, Fluka, and J. T. Baker, respectively. All reagents used were of analytical grade, unless otherwise noted.

2.2. Synthesis of Manganese Oxides. A 0.2028 g portion of $MnSO_4 \cdot H_2O$ was dissolved in 12 mL of distilled deionized water (DDW) at a concentration of 0.1 mol·L^{-1}, and then $KMnO_4$ particles were added into the solution with stirring. The amount of $KMnO_4$ was controlled according to the molar ratio of $KMnO_4/MnSO_4 \cdot H_2O$ as 7:18, 8:17, 9:16, 2:3, and 11:14, respectively. The suspended solutions were subsequently transferred into a Teflon-lined stainless steel autoclave with a volume of about 23 mL, sealed and maintained at 120, 150, and 180 °C for 20 h, respectively. The reaction mixture was then cooled to room temperature and washed by repeated filtration until the filtered solution reached ∼ pH 7, and then dried in an oven at 60 °C. As the procedure used above, 0.1 and 0.2 mol·L^{-1} H_2SO_4, and 0.05 mol·L^{-1} K_2SO_4 solutions were used to substitute for distilled deionized water (DDW), respectively.

To investigate the influence of the complexation of alkyl ammonium salts on the redox reaction, the above $MnSO_4$ solution was first reacted with 0.1 mol·L^{-1} tetramethylammonium bromide (TAB), tetrathylammonium bromide (TEAB), tetrabutylammonium bromide (TBAB) and tetraoctylammonium bromide (TOAB) for 30 min with stirring in a total volume of 12 mL, respectively. $KMnO_4$ particles were then added to the reaction system. The hydrothermal reaction temperatures and $KMnO_4$ concentrations were used as mentioned above.

2.3. Characterization of Manganese Oxides. Synthesized products were identified by X-ray diffraction (XRD) at room temperature using a Scintag XDS 2000 instrument with Cu Kα radiation. The diffractometer was operated at a tube voltage of 45 kV and a tube current of 40 mA. Fourier transform infrared spectroscopy (FTIR, Nicolet 8700) was carried out with a Bruker Equinox 55 model spectrophotometer by making pellets with KBr powder, and the resolution was set at 4 cm^{-1} with a scan number of 15. The morphologies were characterized using a Zeiss DSM 982 Gemini field-emission scanning electron microscope (FESEM). The thermal stability of the samples was determinated with an SDT Q600 thermal gravimetric analysis (TGA) at a heating rate of 4 °C min^{-1}, and TGA analysis was studied in a nitrogen atmosphere. The Brunauer−Emmett−Teller (BET) surface area of manganese oxides was tested with a Quantachrome Autosorb-1-C automated N_2 gas adsorption system. About 0.2 g samples were weighed and degassed at 120 °C for 12 h before N_2 physisorption measurements. Five point measurements were conducted.

The chemical composition of K and Mn in typical samples (K-OMS-2, H-K-OMS-2, and OMS-7) was analyzed as follows: about 50 mg of manganese oxide was dissolved in 2−5 mL concentrated hydrochloric acid solution (36.5%) in a 50 mL Erlenmeyer flask by digestion at 373 K, and the flask was covered by a glass Petri dish with water on top. The solution was subsequently diluted in a two-liter volumetric flask. The concentrations of K and Mn were measured using an inductively coupled plasma atomic emission spectrometry (ICP-AES, Thermo Jarrel Ash).

2.4. Catalytic Performance of Typical Manganese Oxides. To compare the catalytic performance of synthesized OMS-7, K-OMS-2, and H-K-OMS-2, 0.05 g of active manganese oxide after being dried at 120 °C overnight was added to a solution containing 1 mmol of benzyl

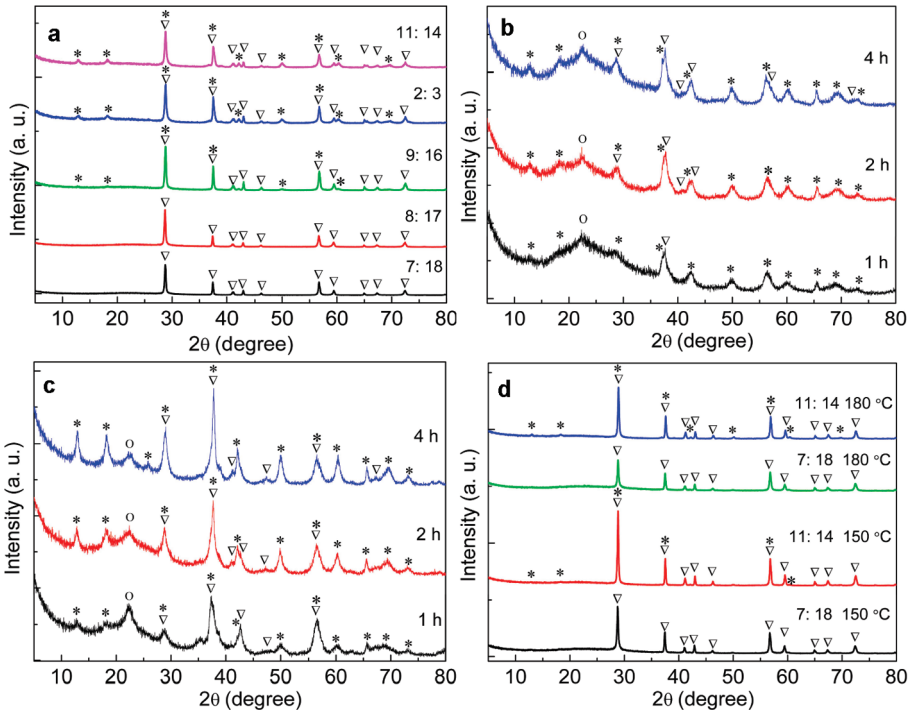

Figure 1. XRD patterns of manganese oxides synthesized in 0.1 mol·L^{-1} $MnSO_4$ solutions with different molar ratios of $KMnO_4/MnSO_4$. (a) 120 °C, 20 h; (b) 7:18, 120 °C; (c) 11:14, 120 °C; (d) 150 and 180 °C for 20 h. OMS-2, OMS-7 and glassy substance are labeled as *, ∇ and O, respectively.

alcohol and 10 mL of toluene placed in a three-necked round-bottom flask connected to a condenser. Subsequently, dry air (after being passed through a drying tube filled with Drierite) was continuously bubbled into the reaction system. The mixture was then stirred with reflux at 120 °C, which was controlled in a paraffin oil bath . After 4 h of reaction, the flask was lifted up above the oil level. The reaction solution was allowed to cool down to room temperature. The catalyst was filtered using a microsyringe fitted with a 0.45 μm inline filter. Finally, the liquid products were analysized using HP 5890 GC, coupled to an HP 5971 mass-selective detector.

2.5. Electrochemical Properties of Typical Manganese Oxides. The electrochemical properties of OMS-7, K-OMS-2, and H-K-OMS-2 were studied by cyclic voltammetry. The working electrode was prepared as follows: 10 mg of manganese oxide, 10 mg of acetylene carbon black and 5 drops of 60% polytetrafluoroethylene solution were ultrasonically dispersed in 5 mL of distilled deionized water, and a 20 μL suspension was pipetted onto a glassy carbon substance. Rolled platinum wire was used as the counter electrode, and a saturated calomel electrode (SCE) was used as a reference electrode with a salt bridge in the experiment.

The working and the counter electrodes were vertically dipped into a 0.1 mol·L^{-1} KOH solution, and O_2 was admitted continuously into the electrolyte for 10 min to saturate the solution. The electrochemical reduction behavior of oxygen was recorded with cyclic voltammetry.

A newly prepared working electrode as described above, a Pt wire counter electrode, and a SCE reference electrode were immersed in a 1.0 mol·L^{-1} Na_2SO_4 solution. The electrochemical capacitive characteristics of OMS-7, K-OMS-2, and H-K-OMS-2 were compared by cyclic voltammetry in a potential window of 0−1.0 V (vs SCE).

3. RESULTS AND DISCUSSION

3.1. Synthesis of Typical Manganese Oxides. *$KMnO_4$−$MnSO_4$ System.* Manganese oxides were fabricated with various molar ratios of $KMnO_4/MnSO_4$,[16,19−21] and the manganese average oxidation state (AOS) could be controlled by adjusting the MnO_4^-/Mn^{2+} ratio.[33] In the present work, the molar ratios of $KMnO_4/MnSO_4$ were used as 7:18, 8:17, 9:16, 2:3, and 11:14 to assume that the manganese AOSs of synthesized samples were 3.4, 3.6, 3.8, 4.0, and 4.2 by calculation, respectively. Figure 1a shows the XRD patterns of manganese oxides prepared with different molar ratios of $KMnO_4/MnSO_4$ in 0.1 mol·L^{-1} $MnSO_4$ solution at 120 °C. The 1 × 1 tunneled OMS-7 (β-MnO_2, JCPDS: 24-0735) material was formed when the ratios were 7:18 and 8:17, respectively. When the ratio increased to 9:16, a mixture of OMS-7 and OMS-2 (cryptomelane, JCPDS: 06-0547) was formed likely because K^+ could be easily accommodated into the 2 × 2 tunnel of manganese oxide, and single phase OMS-2 could be formed by further increasing the molar ratio.[16] The role of K^+ in the formation process of OMS-2 was studied by characterizing products in the initial stage. OMS-2 with a low degree of crystallinity and OMS-7 were generated during the first 4 h of hydrothermal reaction with a 7:18 of MnO_4^-/Mn^{2+} molar ratio, and the diffraction peak of a glassy substance of the sample holder was also observed because of the low yield (Figure 1b). After a 20 h reaction, pure OMS-7 was prepared (Figure 1a) because low crystalline OMS-2 transformed into OMS-7, which has higher thermal stability. The 1 × 2 tunnel structure ramsdellite could be transformed into OMS-7 when the reaction temperature was higher than 150 °C,[34] and OMS-7 could also come from OMS-2 with a low degree of crystallinity without adjusting the pH of the system. High crystalline OMS-2 was formed with high content after 1 h of reaction when the MnO_4^-/Mn^{2+} ratio was increased to 11:14 (Figure 1c). Raising the proportion of $KMnO_4$ facilitated the formation of OMS-2, and K^+ ions possibly participated in the reaction. To investigate the critical role of K^+ in the formation process of OMS-2, K_2SO_4 solutions of 0.05 mol·L^{-1} were added

dx.doi.org/10.1021/cm2011692 |*Chem. Mater.* 2011, 23, 3892–3901

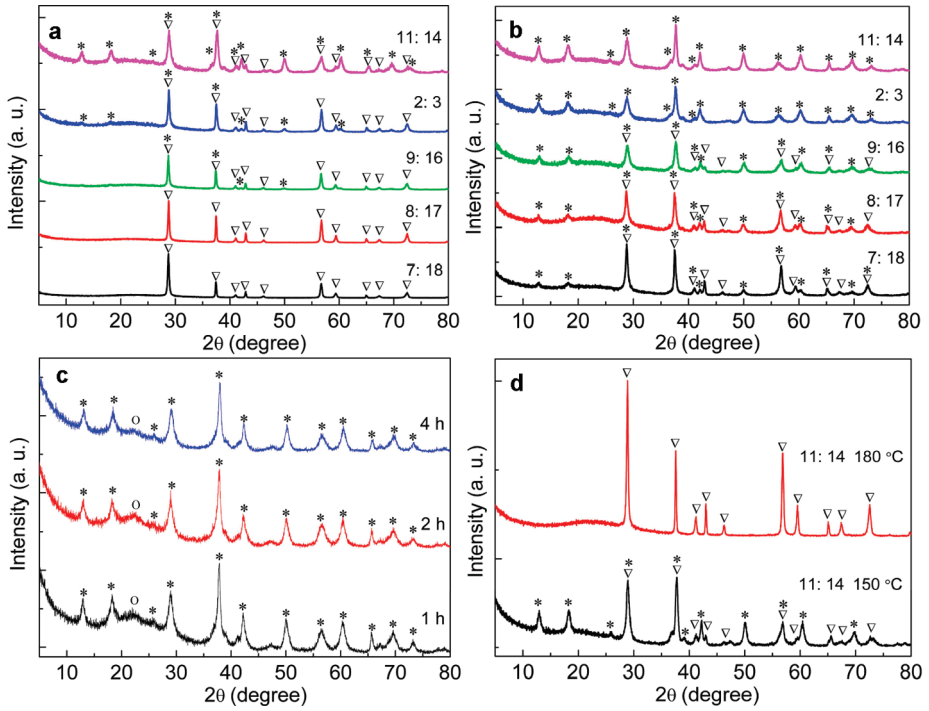

Figure 2. XRD patterns of manganese oxides synthesized in 0.1 mol·L^{-1} $MnSO_4$ with different molar ratios of $KMnO_4/MnSO_4$, additives and temperatures. (a) 0.1 mol·L^{-1} H_2SO_4, 120 °C, 20 h; (b) 0.2 mol·L^{-1} H_2SO_4, 120 °C, 20 h; (c) 11:14, 0.2 mol·L^{-1} H_2SO_4, 120 °C; (d) 11:14, 0.2 mol·L^{-1} H_2SO_4, 20 h. OMS-2, OMS-7 and glassy substance are labeled as *, ∇, and O, respectively.

to the above five systems, respectively, and all the products were characterized to be single-phase OMS-2 (Supporting Information, Figure S1) by hydrothermal reaction at 120 °C for 20 h. This further confirmed the importance of K^+ in this reaction process, which might have acted as a template ion in the formation of the tunnel structure.[15,20]

Layered birnessite was formed first and then transformed into tunnel structures during the formation of tunnel manganese oxides.[16,34,35] However, layered birnessite was not observed in this work. This was possibly due to the rapid transformation of K-birnessite to OMS-2 and OMS-7 because K^+ of a low content in the interlayer can not support the layer. Only when the MnO_4^-/Mn^{2+} ratio increased to 6:1 was K-birnessite formed even at higher temperatures.[16]

The hydrothermal reaction temperature may affect the transformation process of manganese oxide. Figure 1d shows the samples prepared with MnO_4^-/Mn^{2+} ratios of 7:18 and 11:14, respectively. There was no remarkable change in the compositions of products when 150 and 180 °C were employed, respectively.

$KMnO_4$—$MnSO_4$—H_2SO_4 System. The influence of acid concentration on the formation process of layered birnessite to tunnel structure manganese oxide was studied in detail.[18,35] The concentration of H_2SO_4 also played an important role in the hydrothermal reaction of $KMnO_4$ and $MnSO_4$ solutions. When the H_2SO_4 concentration was controlled at 0.1 mol·L^{-1}, there was no obvious difference in the products compared with a reaction system without adding H_2SO_4 when the $KMnO_4/MnSO_4$ ratio was increased from 7:18 to 11:14 (Figure 1a and Figure 2a). When the H_2SO_4 concentration increased to 0.2 mol·L^{-1}, a mixture of OMS-2 and OMS-7 was formed even when the $KMnO_4/MnSO_4$ ratio was as low as 7:18, and the content of OMS-7 decreased with an increase in the $KMnO_4/MnSO_4$ ratio (Figure 2b). The change in OMS-7 content of solid products was indicated by the diffraction peak of OMS-7 at 42.8° (2θ), which decreased and disappeared when the $KMnO_4/MnSO_4$ ratio was increased to 2:3. Pure OMS-2 was generated when the $KMnO_4/MnSO_4$ ratios were used as 2:3 and 11:14 (Figure 2b), suggesting that H^+ ions might enter into the tunnel and support the framework, and prevent the transformation of OMS-2 to OMS-7. There was no OMS-7 in the initial stage (Figure 2c). Because of the small radius of H^+ ions, the 2 × 2 tunnel collapsed when the temperature was increased over 120 °C. OMS-2 partially transformed to OMS-7 at 150 °C and completely into OMS-7 at 180 °C (Figure 2d), which further proved that H^+ ions were partially accommodated in the tunnel.

$KMnO_4$—$MnSO_4$—TBAB System. Organic ammonium ions are used to synthesize layered and unilaminar two-dimensional crystallites of manganese oxides.[22−24] After the complexation reaction of $MnSO_4$ and tetrabutylammonium bromide ($(C_4H_9)_4NBr$, TBAB) for half an hour, the $KMnO_4$ particles were added and dissolved into the solution, and subsequently transferred into the autoclave for 20 h. OMS-2 was formed when the $KMnO_4/MnSO_4$ ratio was increased from 7:18 to 11:14 (Figure 3a). Presumably, TBA^+ complexed with Mn^{2+} to slow the redox reaction of MnO_4^- and Mn^{2+}, which slowed the formation rate of Mn(III) and Mn(IV) oxides and offered enough time for the K^+ ions to insert into the tunnel. A brown precipitate was formed as soon as the $KMnO_4$ particles were put into a single $MnSO_4$ solution. However, the brown precipitate was only formed near the surface of the $KMnO_4$ particles after the complexation reaction of $MnSO_4$ with TBAB for half an hour. Because the product yield was very low before hydrothermal treatment, the precipitate was not collected. After being complexed, TBA^+ ions were distributed around Mn^{2+}, which increased the steric effect for the redox reaction.[25]

dx.doi.org/10.1021/cm2011692 |*Chem. Mater.* 2011, 23, 3892–3901

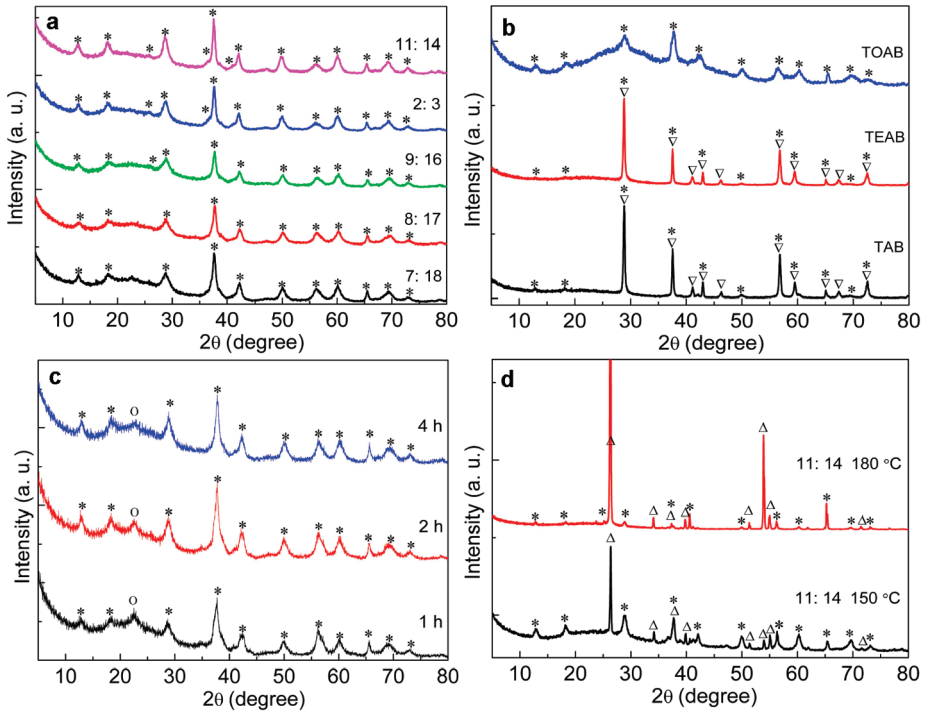

Figure 3. XRD patterns of manganese oxides synthesized in 0.1 mol·L^{-1} $MnSO_4$ with different molar ratios of $KMnO_4/MnSO_4$, time and temperatures. (a) 0.1 mol·L^{-1} TBAB, 120 °C, 20 h; (b) 11:14, 0.1 mol·L^{-1} alkyl ammonium salts, 120 °C, 20 h; (c) 11:14, 0.1 mol·L^{-1} TBAB, 120 °C; (d) 11:14, 0.1 mol·L^{-1} TBAB for 20 h. OMS-2, OMS-7, γ-MnOOH, and glassy substance are labeled as *, ∇, Δ, and O, respectively.

To further investigate the steric effect of the complexation reaction, tetramethylammonium bromide ($(CH_3)_4NBr$, TAB), tetrathylammonium bromide ($(C_2H_5)_4NBr$, TEAB), and tetraoctylammonium bromide ($(C_8H_{17})_4NBr$, TOAB) were used to substitute for TBAB, respectively. A mixture of OMS-7 and OMS-2 was formed when TAB or TEAB were applied (Figure 3b) likely because of weak steric effects owing to the smaller diameters of the quaternary ammonium cations. When TOAB was used in the experiment, poorly crystalline OMS-2 (Figure 3b) was prepared likely because of the greater steric effect for the largest ions of TOA^+.

A certain amount of NH_4^+ is required to stabilize the 2 × 2 tunnels in the formation of OMS-2.[36] The steric effect for the complexation reaction of organic ammonium ions facilitated the formation of OMS-2. OMS-2 was formed at the beginning of the hydrothermal reaction, and the degree of crystallinity was enhanced by prolonging the reaction time (Figure 3c). Organic reagents participated in the redox reaction of $KMnO_4$ and $MnSO_4$, and also had some risk of being oxidized by manganese oxides. When the temperature was increased to 150 °C, OMS-2 and MnOOH (γ-MnOOH, JCPDS: 18-0805) were produced simultaneously (Figure 3d). When temperature was further increased to 180 °C, the intensity of diffraction peaks of MnOOH became strong and sharp, and the composition of OMS-2 decreased even at the $KMnO_4/MnSO_4$ ratio of 11:14. TBAB solution is thermally stable below 180 °C. Tetrabutylammonium bromide acted as an additive to control the morphologies of CeO_2 at 180 °C and Co_3O_4 at 160 °C.[37,38] If TBAB in aqueous solution was thermally decomposed at these temperatures, the morphologies of metal oxides could not be controlled as discussed in the refs 37,38. When 0.1 or 0.2 mol·L^{-1} H_2SO_4 was added to the reaction system with organic TBAB, single-phase OMS-2 could not be formed at 120 °C because of the high oxidation activity of manganese oxides in acidic solution. Therefore, proper temperature and other conditions, such as pH, should be selected when organic reagents were used for the synthesis of manganese oxides.

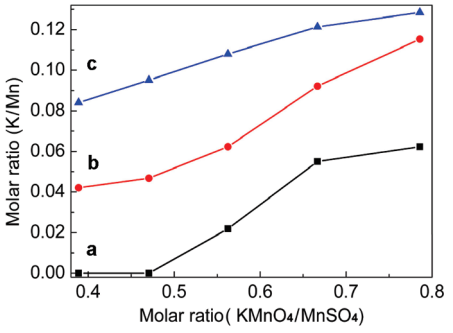

Figure 4. Relationship between molar ratios of K/Mn in synthesized manganese oxides and $KMnO_4/MnSO_4$ in 0.1 mol·L^{-1} $MnSO_4$ solutions at 120 °C for 20 h, (a) without additives; (b) 0.2 mol·L^{-1} H_2SO_4; (c) TBAB.

3.2. Characterization of Typical Manganese Oxides. In the above three reaction systems, the formation mechanism was further proved by the characterization of typical manganese oxides. To make sure that K^+ ions participated in the reaction and tetrabutylammonium cations (TBA^+) were not included in the final structure of OMS-2, the samples were characterized by ICP and FTIR, respectively. Figure 4 shows the relationship between the molar ratios of K/Mn in synthesized manganese oxides and $KMnO_4/MnSO_4$ in 0.1 mol·L^{-1} $MnSO_4$ solutions at 120 °C. Potassium content and molar ratios of K/Mn increased

dx.doi.org/10.1021/cm2011692 |Chem. Mater. 2011, 23, 3892–3901

with the increase of $KMnO_4/MnSO_4$, and a high concentration of K^+ in solution facilitated the formation of OMS-2.[20] The potassium contents of manganese oxides prepared in different reaction systems are in the sequence: $KMnO_4-MnSO_4-TBAB$ > $KMnO_4-MnSO_4-H_2SO_4$ > $KMnO_4-MnSO_4$ with the same $KMnO_4/MnSO_4$ ratio (Figure 4). The content of K in OMS-7 was zero (Figure 4a), which was in agreement with the fact that K^+ can not insert into the 1 × 1 tunnel because of the large ionic diameter. The potassium content in pure OMS-2 prepared in the $KMnO_4-MnSO_4-H_2SO_4$ system was highest with the $KMnO_4/MnSO_4$ ratio of 11:14. However, the $[K^+]$ was lower than that obtained in the $KMnO_4-MnSO_4-TBAB$ system with the same ratio of $KMnO_4/MnSO_4$ (Figure 4b, c). Both K^+ and H^+ are located in the tunnels and support the framework when OMS-2 was prepared in acidic solution because K^+ in the tunnels can be exchanged by H^+ in acidic solution.[1] However, K^+ might be the main composition when produced without adding acid in the reaction system. Therefore, H-K-OMS-2 and K-OMS-2 were formed in the $KMnO_4-MnSO_4-H_2SO_4$ and the $KMnO_4-MnSO_4-TBAB$ systems with a $KMnO_4/MnSO_4$ ratio of 11:14 at 120 °C, respectively.

OMS-7 produced in the $KMnO_4-MnSO_4$ system with a $KMnO_4/MnSO_4$ ratio of 7:18, H-K-OMS-2, and K-OMS-2 were all further characterized and evaluated for physicochemical properties. Figure 5 shows the FTIR spectra of OMS-7, H-K-OMS-2 and K-OMS-2. The characteristic adsorption bands for OMS-7 at 545, 718, and 1106 cm^{-1}, and for OMS-2 at 471, 523, 586, 718, and 3446 cm^{-1} were observed,[39,40] respectively. The dominant absorption peak at 1633 cm^{-1} was assigned to H_2O in the tunnel. However, this peak was not observed for OMS-7, which was further shown by TGA. There was no other absorption peak for TBA^+, which further proved that single-phase K-OMS-2 was formed although TBA^+ participated in the redox reaction, and TBA^+ cations only worked as space-confining additives rather than as template ions.

Typical SEM images for OMS-7, a mixture of OMS-7 and OMS-2 prepared in the $KMnO_4-MnSO_4$ system with a $KMnO_4/MnSO_4$ ratio of 11:14, H-K-OMS-2 and K-OMS-2 are shown in Figure 6. Rodlike nanosized OMS-7 was formed (Figure 6a), and the mixture of OMS-7 and OMS-2 exhibited two different micromorphologies: rodlike and wirelike nanostructures (Figure 6b). H-K-OMS-2 nanowires were formed after adding 0.2 $mol \cdot L^{-1}$ H_2SO_4 with a $KMnO_4/MnSO_4$ ratio of 11:14 (Figure 6c). K-OMS-2 nanobelts were formed by adding TBAB with a $KMnO_4/MnSO_4$ ratio of 11:14, and the length was longer than 1 μm (Figure 6d). Compared with the morphologies in Figure 6a–d, the molar ratio, sulfuric acid, TBAB, and temperature affected the chemical structures, composition, and morphologies of manganese oxides synthesized by a hydrothermal reaction of $KMnO_4$ and $MnSO_4$ solutions. For the above four samples, the specific surface areas were determined to be 14.1, 63.8, 75.7, and 81.8 $m^2\ g^{-1}$, respectively. Nitrogen sorption isotherms of OMS-7, H-K-OMS-2, and K-OMS-2 are shown in the Supporting Information, Figure S2, and some of these data are shown in Table 1.

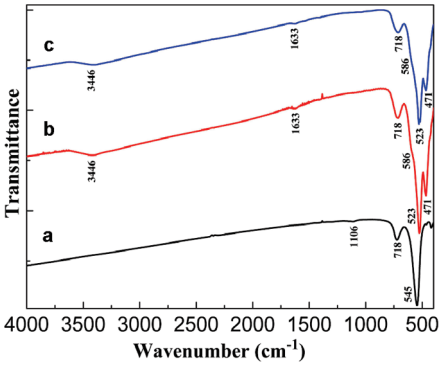

Figure 5. FTIR spectra of the products: (a) OMS-7; (b) H-K-OMS-2; (c) K-OMS-2.

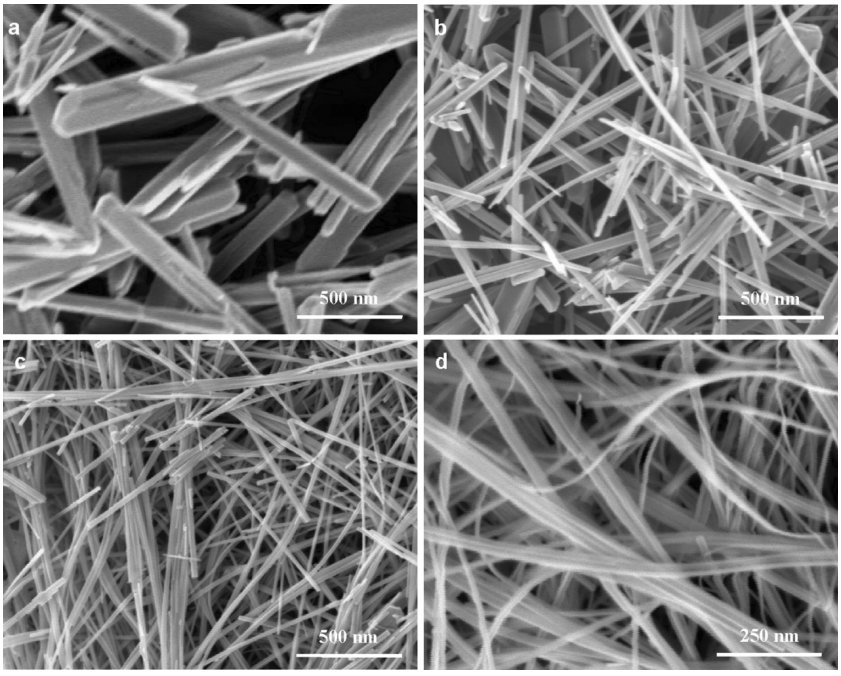

Figure 6. SEM images of synthesized manganese oxides: (a) OMS-7; (b) a mixture of OMS-7 and OMS-2; (c) H-K-OMS-2; (d) K-OMS-2.

dx.doi.org/10.1021/cm2011692 |*Chem. Mater.* 2011, 23, 3892–3901

Table 1. Specific Surface Area and Thermal Analysis of Synthesized Manganese Oxides

		thermal analysis (% mass loss)			
manganese oxide	BET ($m^2 \cdot g^{-1}$)	50−280 (°C)	280−450 (°C)	450−570 (°C)	570−800 (°C)
OMS-7	14.1	0.30	0.37	8.74	3.17
H-K-OMS-2	75.7	1.52	1.18	4.43	4.21
K-OMS-2	81.8	1.66	1.54	3.25	4.71

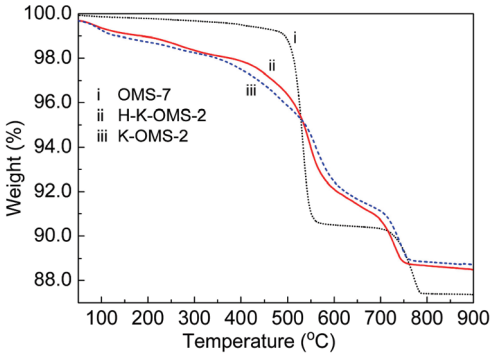

Figure 7. TGA curves of the synthesized manganese oxides.

Lattice oxygen content was measured by thermogravimetric analysis.[13,20,28,29] Figure 7 shows the TGA curves of OMS-7, H-K-OMS-2 and K-OMS-2 in a nitrogen atmosphere with a ramping rate of 4 °C min^{-1}. The profile indicates the corresponding weight losses of O_2 and H_2O in a range of 50−900 °C, which are divided into four steps. (*i*) In the 50−280 °C range, attributed to physisorbed water, the mass loss was not as obvious as reported in ref 13,20,28 and 29 just because all the samples were dried in an oven at 120 °C for over 2 days. (*ii*) In the 280−450 °C range, the mass loss was possibly due to chemisorbed oxygen and water. (*iii*) In the range of 450−570 °C, lattice oxygen was released from manganese oxides. (*iv*) In the range of 570−800 °C, the weight losses were due to the thermal decomposition of Mn(IV) oxides to a lower oxidation state with further evolution of lattice oxygen.[28] The mass loss rates for OMS-7, H-K-OMS-2, and K-OMS-2 in different steps are shown in Table 1. The content of physisorbed water in OMS-7 was about 0.3%, and about 1.6% in H-K-OMS-2 and K-OMS-2, which agreed well with the FTIR results. In the second step, the contents of chemisorbed oxygen and water are in the order of K-OMS-2 > H-K-OMS-2 > OMS-7, and this physicochemical property of manganese oxides shows the exchangeability of oxygen content.[1,13,29] OMS-7 exhibits its main weight loss between 450 and 570 °C, and a less remarkable one above 700 °C (Figure 7 and Table 1) because of the release of oxygen for the transformation to Mn_2O_3 and to Mn_3O_4, respectively.[15,20] In the temperature section of 450−570 °C, H-K-OMS-2 and OMS-7 also released a large amount of lattice oxygen and indicated that the tunnel structure of the K-OMS-2 is not stable.[13,15] The 2 × 2 tunnel framework would collapse when the temperature is over 700 °C.[15] The content of exchangeable active oxygen in the range of 280−450 °C may affect the physicochemical performance of manganese oxides.

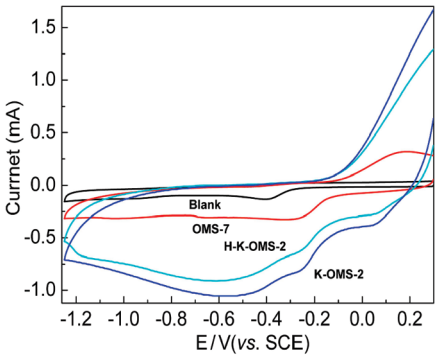

Figure 8. Cyclic voltammograms of prepared manganese oxides in oxygen-saturated 0.1 mol·L^{-1} KOH solution with a scanning rate of 50 mV·s^{-1}.

3.3. Catalytic Performance of Typical Manganese Oxides. Manganese oxides have been used as catalysts for the oxidation of benzyl alcohol to benzaldehyde.[1,20] Content of active lattice oxygen, acidic sites, specific surface area, degree of crystallinity, particle size, and crystal structure influenced the catalytic performance.[1,2,15,20] OMS-7, H-K-OMS-2, and K-OMS-2 were studied as catalysts for the oxidation of benzyl alcohol.

After the catalytic oxidation reaction of benzyl alcohol at 120 °C for 4 h, the conversions of benzyl alcohol to benzaldehyde were 49.3%, 83.3%, and 74.3% when OMS-7, H-K-OMS-2, and K-OMS-2 (Supporting Information, Figure S3) were used, respectively. Exchangeable active oxygen plays an important role in the catalytic oxidation of benzyl alcohol.[1,20] However, Lewis acid sites may provide more opportunities for the adsorption of benzyl alcohol in the first step,[1,28] although K-OMS-2 had a larger specific surface area and higher content of exchangeable active oxygen. OMS-2 prepared in acid solution and K^+ was substituted by H^+ in the tunnel and more acid sites were formed.[1] The elemental analyses of K/Mn in different manganese oxides also supported this exchange process (Figure 4). H-K-OMS-2, K-OMS-2, and OMS-7 exhibited higher catalytic activity than other reports,[20] likely because of the different reaction temperatures, which played an important role in catalytic reactions. In this work, the catalytic reactions were performed at 120 °C, which were higher than 110 °C as reported, although the K-OMS-2 had higher specific surface area as previously reported. Amorphous MnO_2 showed the highest catalytic performance in the reported work suggesting the degree of crystallinity of catalysts was also a very important influence factor for catalytic performance.[20] The low crystallinity OMS-2 synthesized in this work (Figure 3b) might also be a promising catalyst. For the catalytic oxidation reaction of manganese oxides in organic solvents, exchangeable active oxygen was less important than Lewis acid sites.[1] There are some differences in electrochemical properties of these materials in aqueous solutions as described below.

3.4. Electrochemical Properties of Typical Manganese Oxides. Manganese oxides have been widely used and studied as chemical power sources for the electrochemical reduction of oxygen and for supercapacitors. Four electron reduction mechanisms have been proposed in detail; however, the process of oxygen reduction on manganese oxide is not very definitive at present.[11,30,41] Figure 8 shows the cyclic voltammograms of prepared manganese oxides in oxygen-saturated 0.1 mol·L^{-1} KOH solution at a scanning rate of 50 mV·s^{-1}. There are two cathodic current peaks in the range of −0.1 to −0.7 V for

dx.doi.org/10.1021/cm2011692 |*Chem. Mater.* 2011, 23, 3892–3901

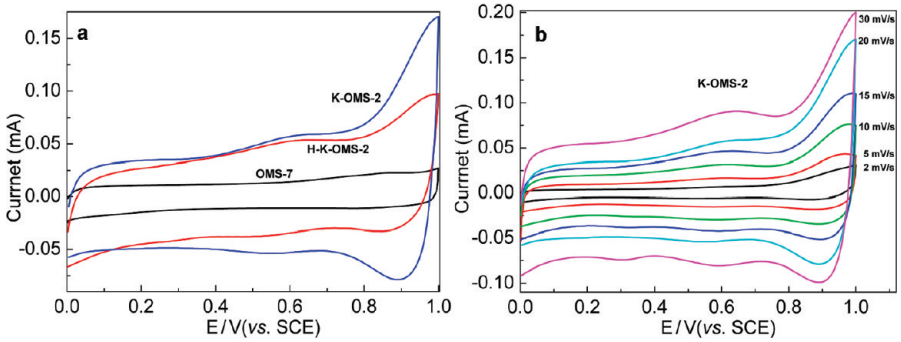

Figure 9. Cyclic voltammograms of prepared manganese oxides in 1.0 mol·L^{-1} Na_2SO_4 solution. (a) Scanning rate: 20 mV·s^{-1}; (b) K-OMS-2 with different scanning rates.

the oxygen adsorption and reduction. The current for oxygen reduction on different manganese oxide electrodes increased in the sequence OMS-7 < H-K-OMS-2 < K-OMS-2. The reduction currents on electrodes of K-OMS-2 and H-K-OMS-2 are significantly higher than those for OMS-7, and K-OMS-2 exhibits superior electroactivity. The specific surface area and exchangeable active oxygen might contribute to the electrocatalytic activity. Each mole of oxygen reduces to produce 4 mol of OH^- ions, and reduction of the adsorbed oxygen accompanying the formation of OH^- is likely to be the rate determining step.[30,41] Large specific surface areas promote the adsorptive capacity for oxygen, and the removal of exchangeable oxygen in the form of OH^- might accelerate the reduction of adsorbed oxygen. Differences in specific surface area and contents of exchangeable oxygen are in the order of K-OMS-2 > H-K-OMS-2 > OMS-7, and the electrocatalytic performance exhibited a similar tendency. However, the specific surface area is not a decisive factor in the electrocatalytic performance of manganese oxides.[11] That is to say, exchangeable active oxygen possibly played a critical role in the electrochemical reduction of oxygen, which could help us understand the differences in electrocatalytic reduction activity of various manganese oxides. Oxygen species with different binding strengths can be probed through the release of oxygen in temperature-programmed desorption (TPD) studies and the reactivity of oxygen with hydrogen or other reductants via temperature-programmed reduction (TPR) methods. Oxygen isotope labeling can be done during the electrocatalytic reactions. The relationship between the content of exchangeable active oxygen species in manganese oxides and reduction rate of oxygen needs to be further investigated in detail.

Figure 9a shows the cyclic voltammograms of OMS-7, H-K-OMS-2, and K-OMS-2 in 1.0 mol·L^{-1} Na_2SO_4 solution. These CVs exhibited pseudocapacitance properties of synthesized H-K-OMS-2 and K-OMS-2, and rectangular and symmetric current—potential current curves for OMS-7. There are two pairs of redox current peaks in the range of 0.4—0.75 V and 0.75—1.0 V. Redox reactions occurred for the deinsertion and insertion of K^+, Na^+, and H^+ in the tunnel sites of OMS-2 during the CV scanning. The capacitance of K-OMS-2 and H-K-OMS-2 was significantly higher than that of OMS-7, which suggested that it was better to use tunnel-structure manganese oxides with a larger size as a pseudocapacitance for the higher capacitance. Although it was reported that specific surface area was not the only factor that determined the electrochemical properties, especially for quasi-capacitance,[42] the capacitance showed a strong correlation with specific surface area of manganese oxides with different structures in this work.

For functional capacitors, the mass transfer rate in solution may affect the capacitance of the active materials. In pseudocapacitance studies of K-OMS-2 and H-K-OMS-2, the transfer rate of H^+ and metal cations (such as K^+ and Na^+) in the tunnel limited the electrochemical properties.[42] The redox current increased with the increase of scanning rate for K-OMS-2 in Na_2SO_4 solution (Figure 9b). However, the capacitance decreased possibly because of the slow diffusion of Na^+ ions into the tunnels of OMS-2. There was some limitation for rapid charge and discharge. To reduce the mass transfer resistance in the tunnels of manganese oxides, cations of electrolyte, such as Li^+, were chosen with a relatively small radius. Comparative studies on the effect of concentration and species of electrolytes on the capacitance of manganese oxide were conducted, and these experiments represented the best capacitance performance in 0.5 mol·L^{-1} LiCl.[8] The influence of electrolyte on capacitance was further clarified in the present work. The charge—discharge cycling for K-OMS-2 and H-K-OMS-2 should be performed at a constant current by using different electrolytes in future studies.

For the oxidation of benzyl alcohol, the catalytic oxidation performance of manganese oxide OMS followed the trend: H-K-OMS-2 > K-OMS-2 > OMS-7. The highest conversion is observed for H-K-OMS-2 because of the larger amount of acid sites in H-K-OMS-2 although K-OMS-2 had a higher content of exchangeable active oxygen, which was studied by isotope labeling.[1] The decreasing order of electrocatalytic reduction of oxygen and supercapacitance properties were in the order K-OMS-2 > H-K-OMS-2 > OMS-7. The difference in physicochemical properties of the above manganese oxides was attributed to the different reaction mechanisms. The catalytic oxidation reactions were carried out in organic solution systems, and Mn^{4+}-type Lewis acid sites played a more important role during the process.[1,28] The electrochemical reactions were conducted in aqueous solution systems. Exchangeable active oxygen in manganese oxide participated in the electrochemical reduction of oxygen gas. For the pseudocapacitance properties of manganese oxides, coupled with the deinsertion/insertion of Na^+ in the tunnels, redox reactions of Mn^{4+}/Mn^{3+} and Mn^{3+}/Mn^{2+} occurred, and specific surface area played an important role during the CV scans.

To increase the catalytic oxidation and electrochemical performance of manganese oxides, crystal structure, degree of crystallinity, specific surface area, and the content of Lewis acid sites and exchangeable active oxygen should be taken into

dx.doi.org/10.1021/cm2011692 |Chem. Mater. 2011, 23, 3892–3901

account. Manganese oxides with a high content of Lewis acid sites possibly have excellent catalytic oxidation activity in nonaqueous solution system. Large-sized tunnel manganese oxides with higher specific surface area exhibited excellent electrochemical properties, such as electrochemical reduction of oxygen and supercapacitance.

4. CONCLUSIONS

Manganese oxide octahedral molecular sieves, OMS-7, H-K-OMS-2, and K-OMS-2, have been successfully prepared by controlling the hydrothermal reaction temperature, the $KMnO_4$/$MnSO_4$ molar ratio, sulfuric acid concentration, and the species of alkyl ammonium salts in 0.1 mol·L^{-1} $MnSO_4$ solution at 120 °C. Only OMS-7 can be formed when $KMnO_4$/$MnSO_4$ molar ratios do not exceed 8:17. A mixture of OMS-7 and K-OMS-2 is formed with a $KMnO_4$/$MnSO_4$ molar ratio in the range of 9:16 to 11:14. H-K-OMS-2 nanowires are formed in 0.2 M H_2SO_4 solution with a $KMnO_4$/$MnSO_4$ molar ratio of 11:14. High and low crystalline K-OMS-2 materials are prepared by adding tetrabutylammonium bromide and tetraoctylammonium bromide into a 0.1 M $MnSO_4$ solution with $KMnO_4$/$MnSO_4$ molar ratio of 11:14, respectively. K^+ ions play an important role in the formation of OMS-2. OMS-7, H-K-OMS-2, and K-OMS-2 are used in the catalytic oxidation of benzyl alcohol to benzaldehyde, and conversion rates are 49.3%, 83.3%, and 74.3%, respectively, and exchangeable active oxygen does not play a very important role in the catalytic performance. However, exchangeable active oxygen greatly contributes to the electrocatalytic performance for oxygen reduction. The electrocatalytic reduction of oxygen and capacitance are in the order K-OMS-2 > H-K-OMS-2 > OMS-7. This work facilitates the preparation of nanosized manganese oxides with different crystal structures and crystallinities and the understanding of the key influencing factors of their catalytic oxidation and electrochemical performance. Physicochemical properties of low crystalline K-OMS-2 and the relationship between exchangeable active oxygen and electrochemical performance of manganese oxides should be investigated in the future.

■ ASSOCIATED CONTENT

Supporting Information. This includes the role of K^+ in the formation of OMS-2, nitrogen sorption isotherms of typical manganese oxides, and catalytic oxidation experiment of OMS-2 and OMS-7. This material is available free of charge via the Internet at http://pubs.acs.org.

■ AUTHOR INFORMATION

Corresponding Author

E-mail: steven.suib@uconn.edu. Phone: 1 860 486 2797. Fax: 1 860 486 2981.

■ ACKNOWLEDGMENT

The authors thank the State Scholarship Fund of China Scholarship Council of the Ministry of Education of China (Grant 2009842329) and the National Natural Science Foundation of China (Grant 20807019) for financial support. We acknowledge the U.S. Department of Energy, Office of Basic Energy Sciences, Division of Chemical, Geochemical and Biological Sciences, for support of this work. The authors also gratefully acknowledge Dr. Frank S. Galasso and Lei Jin at the University of Connecticut for useful suggestions.

■ REFERENCES

(1) Makwana, V. D.; Son, Y. C.; Howell, A. R.; Suib, S. L. *J. Catal.* **2002**, *210*, 46.
(2) Liu, C. S.; Zhang, L. J.; Li, F. B.; Wang, Y.; Gao, Y.; Li, X. Z.; Cao, W. D.; Feng, C. H.; Dong, J.; Sun, L. N. *Ind. Eng. Chem. Res.* **2009**, *48*, 10408.
(3) Huang, H.; Sithambaram, S.; Chen, C. H.; Kithongo, C. K.; Xu, L. P.; Iyer, A.; Garces, H. F.; Suib, S. L. *Chem. Mater.* **2010**, *22*, 3664.
(4) Nogami, M.; Maeda, T.; Uma, T. *Sens. Actuators, B* **2009**, *137*, 603.
(5) Luo, L.; Zhu, H. T.; Liang, J. K.; Rao, G. H.; Li, J. B.; Du, Z. M. *J. Phys. Chem. C* **2010**, *114*, 8782.
(6) Shen, X. F.; Ding, Y. S.; Liu, J.; Han, Z. H.; Budnick, J. I.; Hines, W. A.; Suib, S. L. *J. Am. Chem. Soc.* **2005**, *127*, 6166.
(7) Lee, S. W.; Kim, J.; Chen, S.; Hammond, P. T.; Shao-Horn, Y. *ACS Nano* **2010**, *4*, 3889.
(8) Wu, M. Q.; Snook, G. A.; Chen, G. C.; Fray, D. J. *Electrochem. Commun.* **2004**, *6*, 499.
(9) Song, C. H.; Li, R. Q.; Liu, F.; Feng, X. H.; Tan, W. F.; Qiu, G. H. *Electrochim. Acta* **2010**, *55*, 9157.
(10) Suib, S. L. *Acc. Chem. Res.* **2008**, *41*, 479.
(11) Xiao, W.; Wang, D. L.; Lou, X. W. *J. Phys. Chem. C* **2010**, *114*, 1694–1700.
(12) Yuan, J. K.; Li, W. N.; Gomez, S.; Suib, S. L. *J. Am. Chem. Soc.* **2005**, *127*, 14184.
(13) Chen, X.; Shen, Y. F.; Suib, S. L.; O'Young, C. L. *Chem. Mater.* **2002**, *14*, 940.
(14) Polverejan, M.; Villegas, J. C.; Suib, S. L. *J. Am. Chem. Soc.* **2004**, *126*, 7774.
(15) Ding, Y. S.; Shen, X. F.; Sithambaram, S.; Gomez, S.; Kumar, R.; Crisostomo, V. M. B.; Suib, S. L.; Aindow, M. S. *Chem. Mater.* **2005**, *17*, 5382.
(16) Wang, X.; Li, Y. D. *Chem.—Eur. J.* **2003**, *9*, 300.
(17) Sinha, A. K.; Basu, M.; Pradhan, M.; Sarkar, S.; Negishi, Y.; Pal, T. *J. Phys. Chem. C* **2010**, *114*, 21173.
(18) Zhang, Q.; Xiao, Z. D.; Feng, X. H.; Tan, W. F.; Qiu, G. H.; Liu, F. *Mater. Chem. Phys.* **2011**, *125*, 678.
(19) DeGuzman, R. N.; Shen, Y. F.; Neth, E. J.; Suib, S. L.; O'Young, C. L.; Levine, S.; Newsam, J. M. *Chem. Mater.* **1994**, *6*, 815.
(20) Schurz, F.; Bauchert, J. M.; Merker, T.; Schleid, T.; Hasse, H.; Gläser, R. *Appl. Catal., A* **2009**, *355*, 42.
(21) Portehault, D.; Cassaignon, S.; Baudrin, E.; Jolivet, J. P. *Chem. Mater.* **2007**, *19*, 5410.
(22) Gao, Q. M.; Giraldo, O.; Tong, W.; Suib, S. L. *Chem. Mater.* **2001**, *13*, 778.
(23) Omomo, Y.; Sasaki, T.; Wang, L. Z.; Watanabe, M. *J. Am. Chem. Soc.* **2003**, *125*, 3568.
(24) Nakayama, M.; Konishi, S.; Tagashira, H.; Ogura, K. *Langmuir* **2005**, *21*, 354.
(25) Tong, W.; Xia, G. G.; Tian, Z. R.; Liu, J.; Cai, J.; Suib, S. L.; Hanson, J. C. *Chem. Mater.* **2002**, *14*, 615.
(26) Thoma, S. G.; Bonhomme, F.; Cygan, R. T. *Chem. Mater.* **2004**, *16*, 2068.
(27) Xiong, Y. J.; Xie, Y.; Li, Z. Q.; Wu, C. Z. *Chem.—Eur. J.* **2003**, *9*, 1645.
(28) Li, J. H.; Wang, R. H.; Hao, J. M. *J. Phys. Chem. C* **2010**, *114*, 10544.
(29) Rebello, J. S.; Samant, P. V.; Figueiredo, J. L.; Fernandes, J. B. *J. Power Sources* **2006**, *153*, 36.
(30) Cao, Y. L.; Yang, H. X.; Ai, X. P.; Xiao, L. F. *J. Electroanal. Chem.* **2003**, *557*, 127.
(31) Ghodbane, O.; Pascal, J. L.; Favier, F. *ACS Appl. Mater. Interfaces* **2009**, *1*, 1130.

(32) Donne, S. W.; Hollenkamp, A. F.; Jones, B. C. *J. Power Sources* **2010**, *195*, 367.
(33) Cui, H. J.; Qiu, G. H.; Feng, X. H.; Tan, W. F.; Liu, F. *Clays Clay Miner.* **2009**, *57*, 715.
(34) Shen, X. F.; Ding, Y. S.; Hanson, J. C.; Aindow, M.; Suib, S. L. *J. Am. Chem. Soc.* **2006**, *128*, 4570.
(35) Shen, X. F.; Ding, Y. S.; Liu, J.; Cai, J.; Laubernds, K.; Zerger, R. P.; Vasiliev, A.; Aindow, M.; Suib, S. L. *Adv. Mater.* **2005**, *17*, 805.
(36) Wang, X.; Li, Y. D. *J. Am. Chem. Soc.* **2002**, *124*, 2280.
(37) Zhong, L. S.; Hu, J. S.; Cao, A. M.; Liu, Q.; Song, W. G.; Wan, L. J. *Chem. Mater.* **2007**, *19*, 1648.
(38) Li, L. L.; Chu, Y.; Liu, Y.; Song, J. J.; Wang, D.; Du, X. W. *Mater. Lett.* **2008**, *62*, 1507.
(39) Julien, C. M.; Massot, M.; Poinsignon, C. *Spectrochim. Acta, Part A* **2004**, *60*, 689.
(40) Zhang, L. C.; Liu, Z. H.; Tang, X. H.; Wang, J. F.; Ooi, K. *Mater. Res. Bull.* **2007**, *42*, 1432.
(41) Roche, I.; Chaînet, E.; Chatenet, M.; Vondrák, J. *J. Phys. Chem. C* **2007**, *111*, 1434.
(42) Subramanian, V.; Zhu, H. W.; Vajtai, R.; Ajayan, P. M.; Wei, B. Q. *J. Phys. Chem. B* **2005**, *109*, 20207.